

Today's Outline - November 16, 2016

Today's Outline - November 16, 2016

- Resonant and inelastic techniques

Today's Outline - November 16, 2016

- Resonant and inelastic techniques
 - Diffraction anomalous fine structure

Today's Outline - November 16, 2016

- Resonant and inelastic techniques
 - Diffraction anomalous fine structure
 - X-ray Raman spectroscopy

Today's Outline - November 16, 2016

- Resonant and inelastic techniques
 - Diffraction anomalous fine structure
 - X-ray Raman spectroscopy
 - Resonant inelastic x-ray scattering

Today's Outline - November 16, 2016

- Resonant and inelastic techniques
 - Diffraction anomalous fine structure
 - X-ray Raman spectroscopy
 - Resonant inelastic x-ray scattering
 - X-ray emission spectroscopy

Today's Outline - November 16, 2016

- Resonant and inelastic techniques
 - Diffraction anomalous fine structure
 - X-ray Raman spectroscopy
 - Resonant inelastic x-ray scattering
 - X-ray emission spectroscopy

Homework Assignment #7:

Chapter 7: 2,3,9,10,11

due Monday, November 28, 2016

Today's Outline - November 16, 2016

- Resonant and inelastic techniques
 - Diffraction anomalous fine structure
 - X-ray Raman spectroscopy
 - Resonant inelastic x-ray scattering
 - X-ray emission spectroscopy

Homework Assignment #7:

Chapter 7: 2,3,9,10,11

due Monday, November 28, 2016

Final Exam, Wednesday, December 7, 2016, Stuart Building 213

2 sessions: 09:00-12:00; 13:00-17:00; (this may change)

Today's Outline - November 16, 2016

- Resonant and inelastic techniques
 - Diffraction anomalous fine structure
 - X-ray Raman spectroscopy
 - Resonant inelastic x-ray scattering
 - X-ray emission spectroscopy

Homework Assignment #7:

Chapter 7: 2,3,9,10,11

due Monday, November 28, 2016

Final Exam, Wednesday, December 7, 2016, Stuart Building 213

2 sessions: 09:00-12:00; 13:00-17:00; (this may change)

Provide me with the paper you intend to present and a preferred session for the exam

Today's Outline - November 16, 2016

- Resonant and inelastic techniques
 - Diffraction anomalous fine structure
 - X-ray Raman spectroscopy
 - Resonant inelastic x-ray scattering
 - X-ray emission spectroscopy

Homework Assignment #7:

Chapter 7: 2,3,9,10,11

due Monday, November 28, 2016

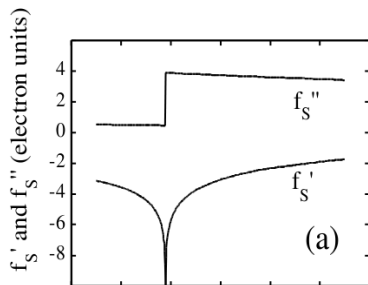
Final Exam, Wednesday, December 7, 2016, Stuart Building 213

2 sessions: 09:00-12:00; 13:00-17:00; (this may change)

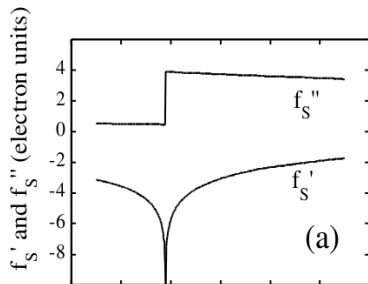
Provide me with the paper you intend to present and a preferred session for the exam

Send me your presentation in Powerpoint or PDF format before before your session

Diffraction anomalous fine structure (DAFS)

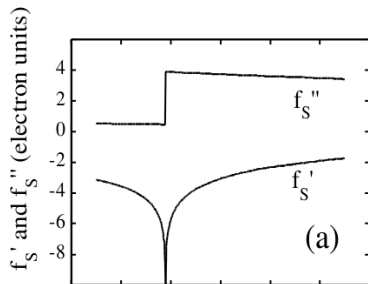


Diffraction anomalous fine structure (DAFS)



The real part of scattering factor of an atom has a resonance at the absorption edge

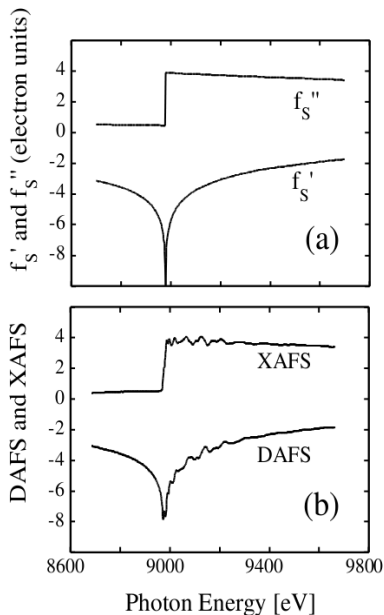
Diffraction anomalous fine structure (DAFS)



The real part of scattering factor of an atom has a resonance at the absorption edge

An atom in a real solid or liquid shows EXAFS oscillations in the absorption cross section which are reflected in the resonant term as well

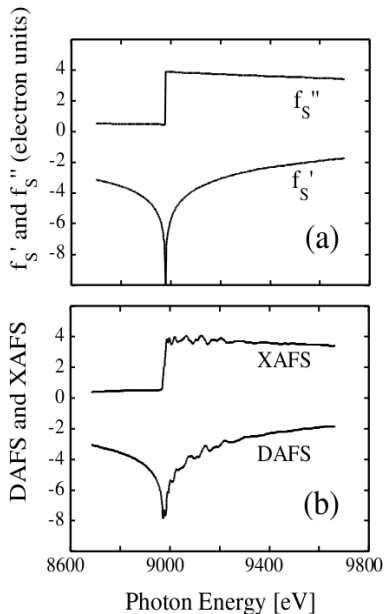
Diffraction anomalous fine structure (DAFS)



The real part of scattering factor of an atom has a resonance at the absorption edge

An atom in a real solid or liquid shows EXAFS oscillations in the absorption cross section which are reflected in the resonant term as well

Diffraction anomalous fine structure (DAFS)

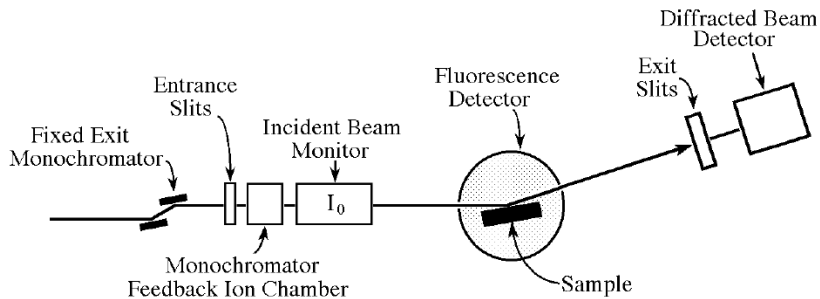


The real part of scattering factor of an atom has a resonance at the absorption edge

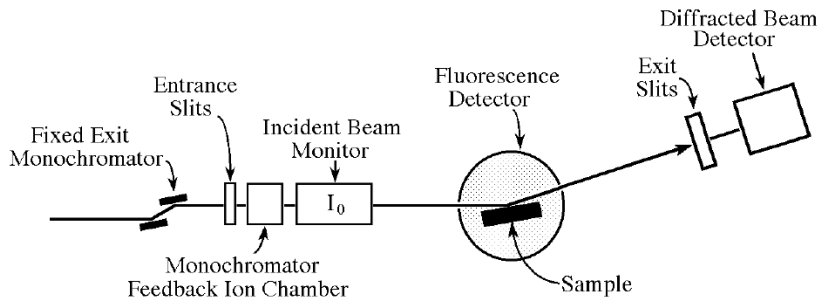
An atom in a real solid or liquid shows EXAFS oscillations in the absorption cross section which are reflected in the resonant term as well

This can be measured in Bragg reflections contributed to by the atom with the absorption edge and exploited to extract site specific information

The DAFS experiment

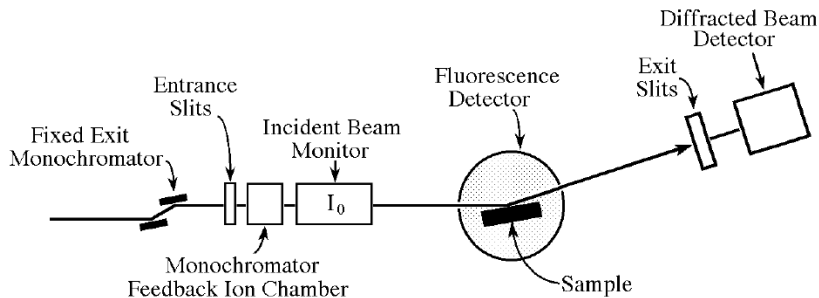


The DAFS experiment



As the energy is swept through the absorption edge, the angle of the sample and the detector are changed to remain in a Bragg condition.

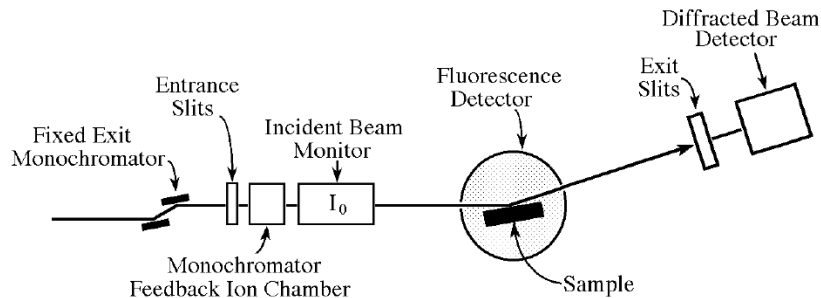
The DAFS experiment



As the energy is swept through the absorption edge, the angle of the sample and the detector are changed to remain in a Bragg condition.

Several peaks are measured to be able to extract information about individual atomic sites.

The DAFS experiment

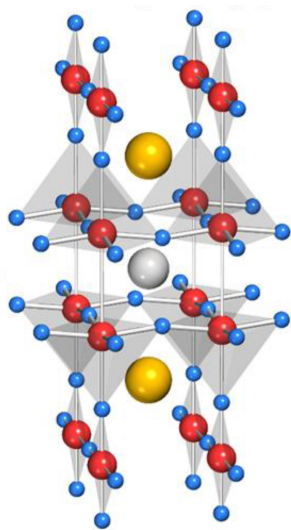


As the energy is swept through the absorption edge, the angle of the sample and the detector are changed to remain in a Bragg condition.

Several peaks are measured to be able to extract information about individual atomic sites.

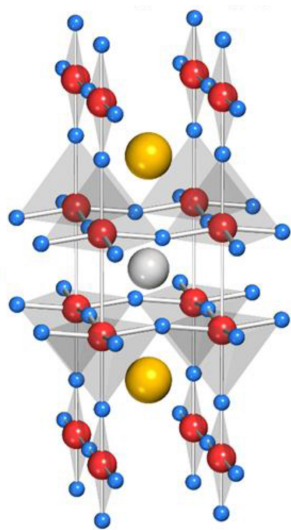
Initially experiments were done on single crystals but now DAFS on powders can be performed

DAFS of $\text{YBa}_2\text{Cu}_3\text{O}_7$



'Separated anomalous scattering amplitudes for the inequivalent Cu sites in $\text{YBa}_2\text{Cu}_3\text{O}_{7-\delta}$ using DAFS,' J.O. Cross, M. Newville, L.B. Sorensen, H.J. Straiger, C.E. Bouldin, and J.C. Woicik, *J. Phys.* **C2**, 745-747 (1997).

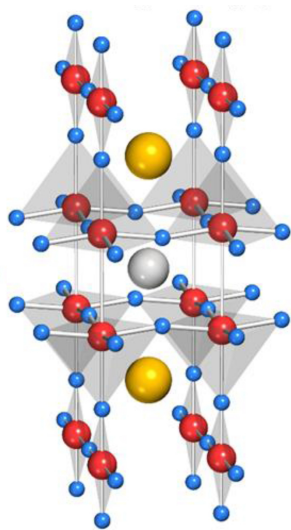
DAFS of $\text{YBa}_2\text{Cu}_3\text{O}_7$



$\text{YBa}_2\text{Cu}_3\text{O}_{7-\delta}$ is a defect perovskite structure with two distinct copper sites

'Separated anomalous scattering amplitudes for the inequivalent Cu sites in $\text{YBa}_2\text{Cu}_3\text{O}_{7-\delta}$ using DAFS,' J.O. Cross, M. Newville, L.B. Sorensen, H.J. Straiger, C.E. Bouldin, and J.C. Woicik, *J. Phys.* **C2**, 745-747 (1997).

DAFS of $\text{YBa}_2\text{Cu}_3\text{O}_7$

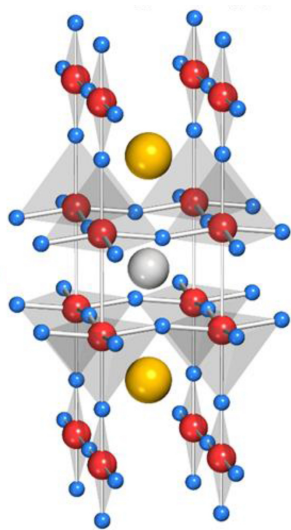


$\text{YBa}_2\text{Cu}_3\text{O}_{7-\delta}$ is a defect perovskite structure with two distinct copper sites

the two Cu sites have distinct local environments, one has square-pyramidal coordination and the second has square planar

'Separated anomalous scattering amplitudes for the inequivalent Cu sites in $\text{YBa}_2\text{Cu}_3\text{O}_{7-\delta}$ using DAFS,' J.O. Cross, M. Newville, L.B. Sorensen, H.J. Straiger, C.E. Bouldin, and J.C. Woicik, *J. Phys. C2*, 745-747 (1997).

DAFS of $\text{YBa}_2\text{Cu}_3\text{O}_7$



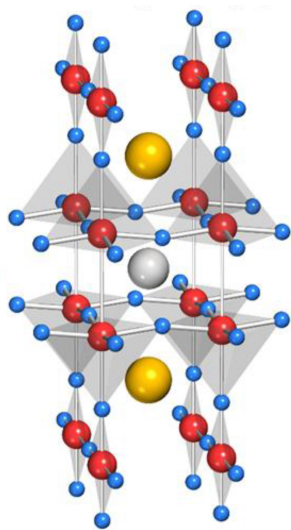
$\text{YBa}_2\text{Cu}_3\text{O}_{7-\delta}$ is a defect perovskite structure with two distinct copper sites

the two Cu sites have distinct local environments, one has square-pyramidal coordination and the second has square planar

with simple EXAFS, you will see a superposition of the two sites in a 2:1 ratio

'Separated anomalous scattering amplitudes for the inequivalent Cu sites in $\text{YBa}_2\text{Cu}_3\text{O}_{7-\delta}$ using DAFS,' J.O. Cross, M. Newville, L.B. Sorensen, H.J. Straiger, C.E. Bouldin, and J.C. Woicik, *J. Phys.* **C2**, 745-747 (1997).

DAFS of $\text{YBa}_2\text{Cu}_3\text{O}_7$



$\text{YBa}_2\text{Cu}_3\text{O}_{7-\delta}$ is a defect perovskite structure with two distinct copper sites

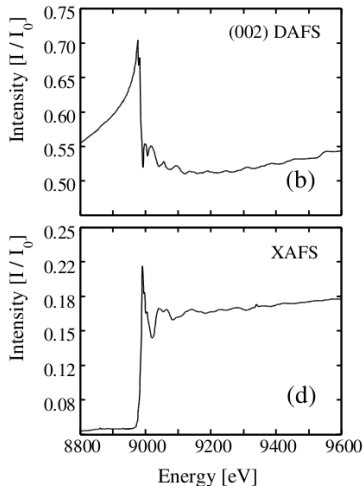
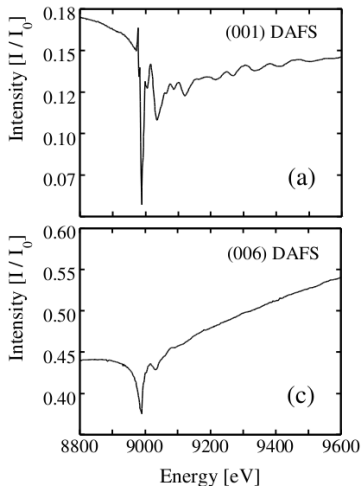
the two Cu sites have distinct local environments, one has square-pyramidal coordination and the second has square planar

with simple EXAFS, you will see a superposition of the two sites in a 2:1 ratio

by measuring the DAFS of multiple diffraction peaks, it is possible to separate the EXAFS of the two Cu sites

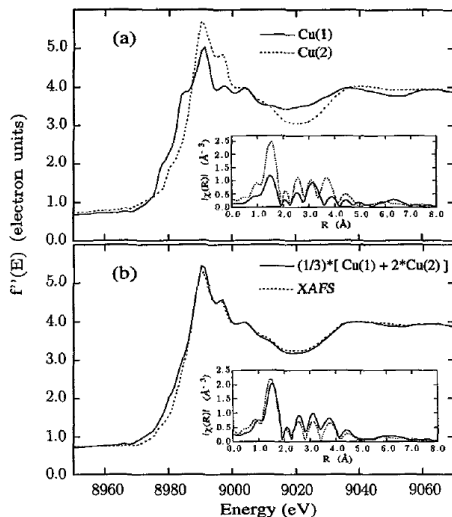
'Separated anomalous scattering amplitudes for the inequivalent Cu sites in $\text{YBa}_2\text{Cu}_3\text{O}_{7-\delta}$ using DAFS,' J.O. Cross, M. Newville, L.B. Sorensen, H.J. Straiger, C.E. Bouldin, and J.C. Woicik, *J. Phys.* **C2**, 745-747 (1997).

DAFS of $\text{YBa}_2\text{Cu}_3\text{O}_7$



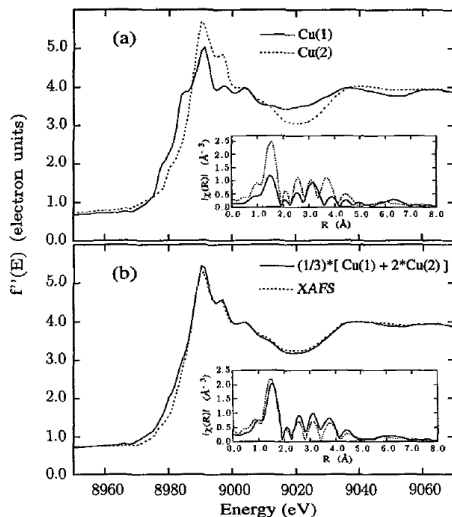
'Separated anomalous scattering amplitudes for the inequivalent Cu sites in $\text{YBa}_2\text{Cu}_3\text{O}_{7-\delta}$ using DAFS," J.O. Cross, M. Newville, L.B. Sorensen, H.J. Straiger, C.E. Bouldin, and J.C. Woicik, *J. Phys. C2*, 745-747 (1997).

DAFS of $\text{YBa}_2\text{Cu}_3\text{O}_7$



'Separated anomalous scattering amplitudes for the inequivalent Cu sites in $\text{YBa}_2\text{Cu}_3\text{O}_{7-\delta}$ using DAFS,' J.O. Cross, M. Newville, L.B. Sorensen, H.J. Straiger, C.E. Bouldin, and J.C. Woicik, *J. Phys.* C2, 745-747 (1997).

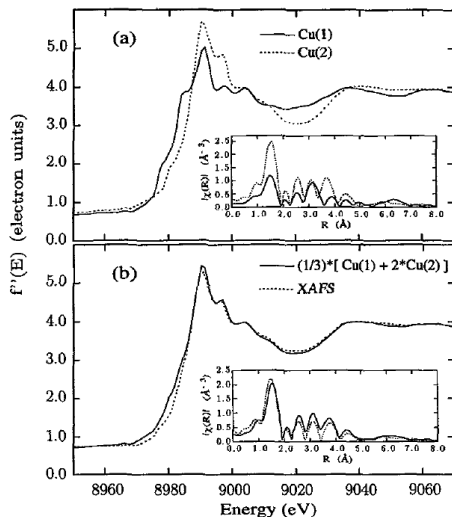
DAFS of $\text{YBa}_2\text{Cu}_3\text{O}_7$



The two Cu sites are distinctly different in both edge position and shape

'Separated anomalous scattering amplitudes for the inequivalent Cu sites in $\text{YBa}_2\text{Cu}_3\text{O}_{7-\delta}$ using DAFS,' J.O. Cross, M. Newville, L.B. Sorensen, H.J. Straiger, C.E. Bouldin, and J.C. Woicik, *J. Phys. C2*, 745-747 (1997).

DAFS of $\text{YBa}_2\text{Cu}_3\text{O}_7$

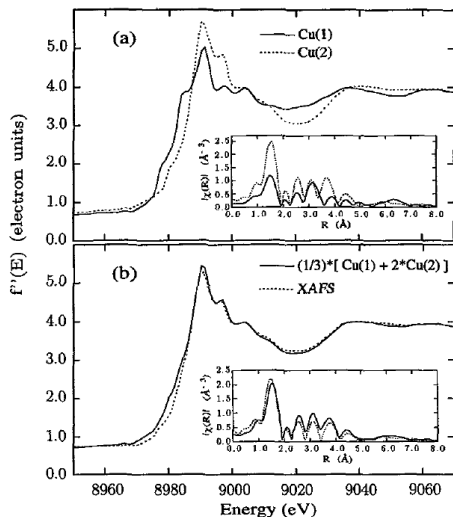


The two Cu sites are distinctly different in both edge position and shape

the Fourier transform is also significantly different for the two sites, particularly the amplitude of the Cu-O peak in the real-space EXAFS

'Separated anomalous scattering amplitudes for the inequivalent Cu sites in $\text{YBa}_2\text{Cu}_3\text{O}_{7-\delta}$ using DAFS,' J.O. Cross, M. Newville, L.B. Sorensen, H.J. Straiger, C.E. Bouldin, and J.C. Woicik, *J. Phys.* C2, 745-747 (1997).

DAFS of $\text{YBa}_2\text{Cu}_3\text{O}_7$



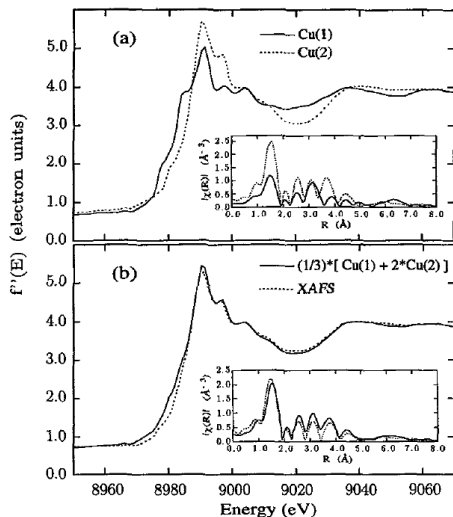
The two Cu sites are distinctly different in both edge position and shape

the Fourier transform is also significantly different for the two sites, particularly the amplitude of the Cu-O peak in the real-space EXAFS

combined in the 2:1 ratio, the measured EXAFS is recovered

'Separated anomalous scattering amplitudes for the inequivalent Cu sites in $\text{YBa}_2\text{Cu}_3\text{O}_{7-\delta}$ using DAFS,' J.O. Cross, M. Newville, L.B. Sorensen, H.J. Straiger, C.E. Bouldin, and J.C. Woicik, *J. Phys.* C2, 745-747 (1997).

DAFS of $\text{YBa}_2\text{Cu}_3\text{O}_7$



The two Cu sites are distinctly different in both edge position and shape

the Fourier transform is also significantly different for the two sites, particularly the amplitude of the Cu-O peak in the real-space EXAFS

combined in the 2:1 ratio, the measured EXAFS is recovered

This data was taken on a single crystal but it is also possible to measure powders using DAFS

'Separated anomalous scattering amplitudes for the inequivalent Cu sites in $\text{YBa}_2\text{Cu}_3\text{O}_{7-\delta}$ using DAFS,' J.O. Cross, M. Newville, L.B. Sorensen, H.J. Straiger, C.E. Bouldin, and J.C. Woicik, *J. Phys. C2*, 745-747 (1997).

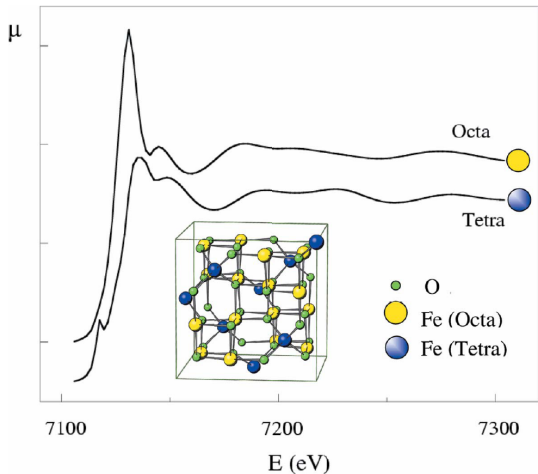
DAFS of maghemite $\gamma\text{-Fe}_2\text{O}_3$

In this study, a mixed phase material with Fe in both phases, is measured and the two sites of the maghemite ($\gamma\text{-Fe}_2\text{O}_3$) are separated

"Diffraction anomalous fine structure study of iron/iron oxide nanoparticles,"
C. Meneghini, F. Boscherini, L. Pasquini, and H. Renevier, *J. Appl. Cryst.*
42, 642-645 (2009)

DAFS of maghemite $\gamma\text{-Fe}_2\text{O}_3$

In this study, a mixed phase material with Fe in both phases, is measured and the two sites of the maghemite ($\gamma\text{-Fe}_2\text{O}_3$) are separated

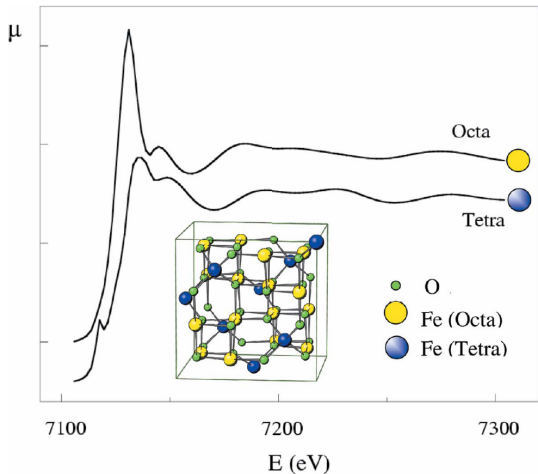


"Diffraction anomalous fine structure study of iron/iron oxide nanoparticles,"
C. Meneghini, F. Boscherini, L. Pasquini, and H. Renevier, *J. Appl. Cryst.*
42, 642-645 (2009)

DAFS of maghemite $\gamma\text{-Fe}_2\text{O}_3$

In this study, a mixed phase material with Fe in both phases, is measured and the two sites of the maghemite ($\gamma\text{-Fe}_2\text{O}_3$) are separated

one of the Fe sites is octahedral and the other tetrahedral



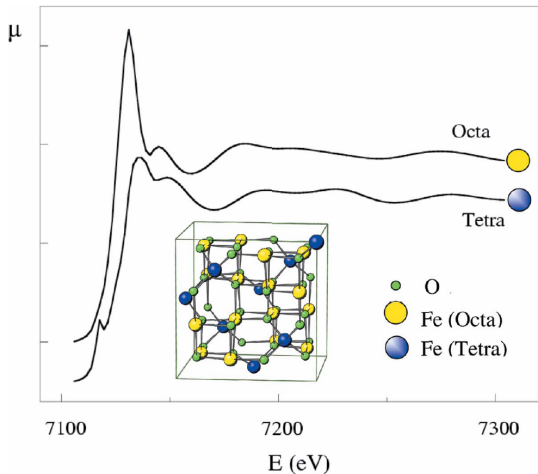
"Diffraction anomalous fine structure study of iron/iron oxide nanoparticles,"
C. Meneghini, F. Boscherini, L. Pasquini, and H. Renevier, *J. Appl. Cryst.*
42, 642-645 (2009)

DAFS of maghemite $\gamma\text{-Fe}_2\text{O}_3$

In this study, a mixed phase material with Fe in both phases, is measured and the two sites of the maghemite ($\gamma\text{-Fe}_2\text{O}_3$) are separated

one of the Fe sites is octahedral and the other tetrahedral

DAFS can also be used to separate different phases which contain the same element in a heterogeneous system or closely overlapping absorption edges



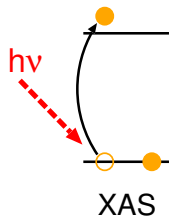
"Diffraction anomalous fine structure study of iron/iron oxide nanoparticles,"
C. Meneghini, F. Boscherini, L. Pasquini, and H. Renevier, *J. Appl. Cryst.*
42, 642-645 (2009)

X-ray Raman (XRR)

X-ray Raman is a way to measure the XAS spectrum of light elements whose absorption edges are below 2 keV.

X-ray Raman (XRR)

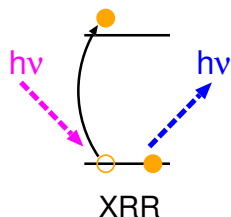
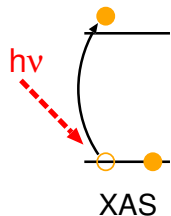
X-ray Raman is a way to measure the XAS spectrum of light elements whose absorption edges are below 2 keV.



The x-ray absorption event consists of the absorption of a photon and production of a photoelectron

X-ray Raman (XRR)

X-ray Raman is a way to measure the XAS spectrum of light elements whose absorption edges are below 2 keV.

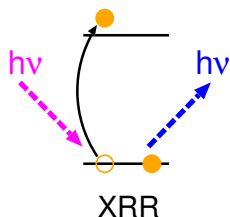
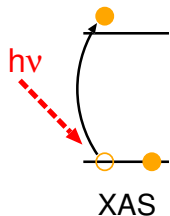


The x-ray absorption event consists of the absorption of a photon and production of a photoelectron

X-ray Raman is a similar process which produces a photoelectron but is an inelastic scattering process with an outgoing photon of lower energy

X-ray Raman (XRR)

X-ray Raman is a way to measure the XAS spectrum of light elements whose absorption edges are below 2 keV.



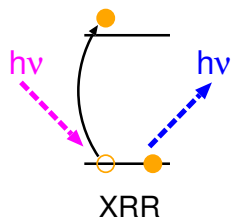
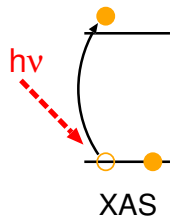
The x-ray absorption event consists of the absorption of a photon and production of a photoelectron

X-ray Raman is a similar process which produces a photoelectron but is an inelastic scattering process with an outgoing photon of lower energy

The incoming x-rays are high energy and the detector is set to measure outgoing x-rays which are at a fixed energy.

X-ray Raman (XRR)

X-ray Raman is a way to measure the XAS spectrum of light elements whose absorption edges are below 2 keV.

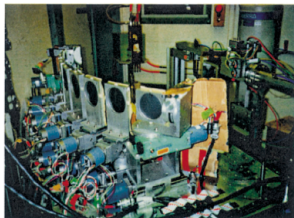
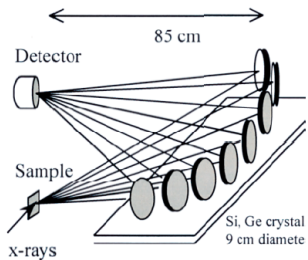


The x-ray absorption event consists of the absorption of a photon and production of a photoelectron

X-ray Raman is a similar process which produces a photoelectron but is an inelastic scattering process with an outgoing photon of lower energy

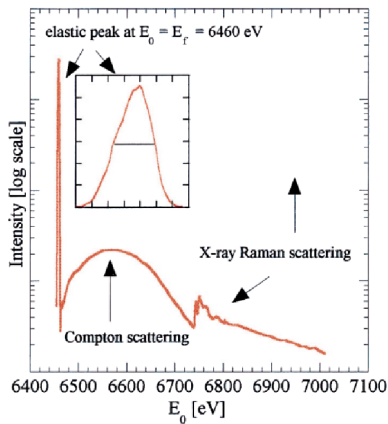
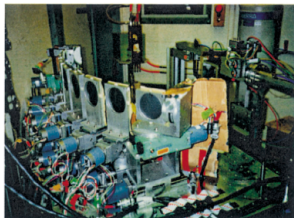
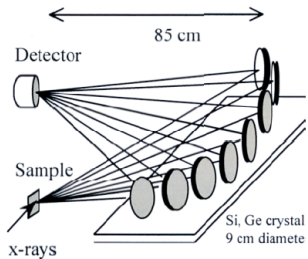
The incoming x-rays are high energy and the detector is set to measure outgoing x-rays which are at a fixed energy. The incoming energy is scanned and the processes detected depend on the difference in energy

The XRR experiment



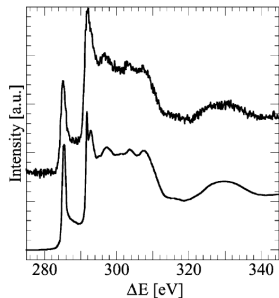
"Bulk-sensitive XAS characterization of light elements: from x-ray Raman scattering to x-ray Raman spectroscopy," U. Bergmann, P. Glatzel, and S. Cramer, *Microchem. J.* **71**, 221-230 (2002)

The XRR experiment



"Bulk-sensitive XAS characterization of light elements: from x-ray Raman scattering to x-ray Raman spectroscopy," U. Bergmann, P. Glatzel, and S. Cramer, *Microchem. J.* **71**, 221-230 (2002)

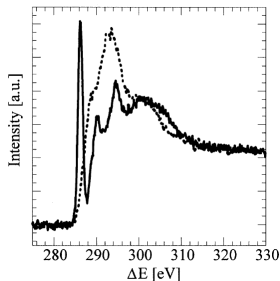
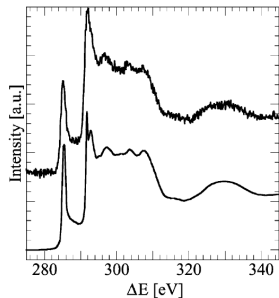
XRR spectra of light elements



Comparison of XRR and XAS on graphite

"Bulk-sensitive XAS characterization of light elements: from x-ray Raman scattering to x-ray Raman spectroscopy," U. Bergmann, P. Glatzel, and S. Cramer, *Microchem. J.* **71**, 221-230 (2002)

XRR spectra of light elements

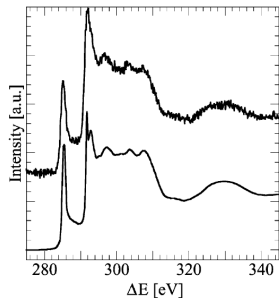


Comparison of XRR
and XAS on graphite

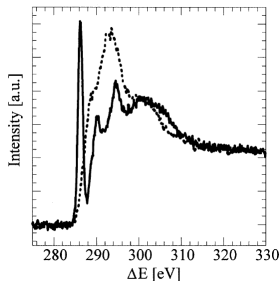
Aromatic (solid) and
aliphatic (dashed) car-
bon K-edge x-ray Ra-
man spectra

"Bulk-sensitive XAS characterization of light elements: from x-ray Raman scattering to x-ray Raman spectroscopy," U. Bergmann, P. Glatzel, and S. Cramer, *Microchem. J.* **71**, 221-230 (2002)

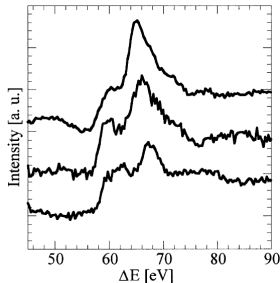
XRR spectra of light elements



Comparison of XRR and XAS on graphite



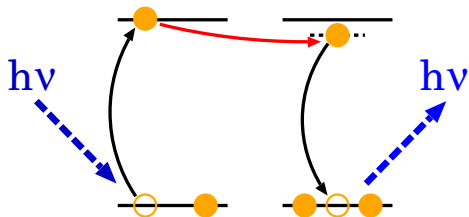
Aromatic (solid) and aliphatic (dashed) carbon K-edge x-ray Raman spectra



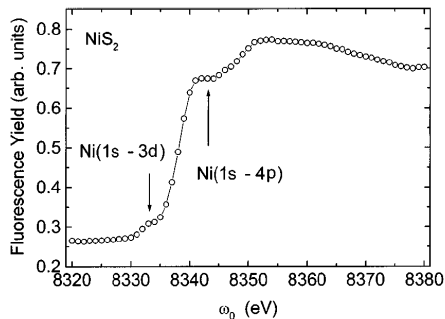
Li K-edge spectra for LiOH·H₂O (top), Li₂CO₃ (middle), and Li₄SiO₄ (bottom).

"Bulk-sensitive XAS characterization of light elements: from x-ray Raman scattering to x-ray Raman spectroscopy," U. Bergmann, P. Glatzel, and S. Cramer, *Microchem. J.* **71**, 221-230 (2002)

Resonant inelastic x-ray scattering (RIXS)

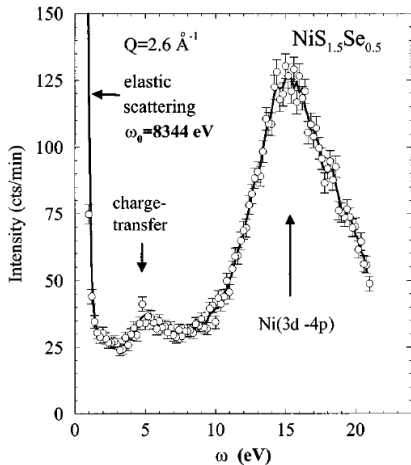
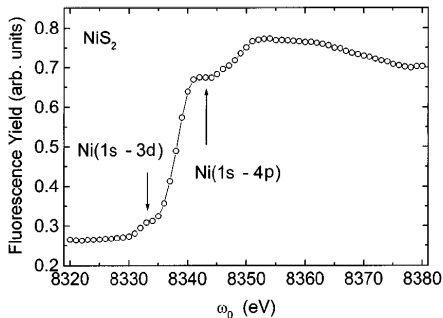


RIXS measures electronic excitations



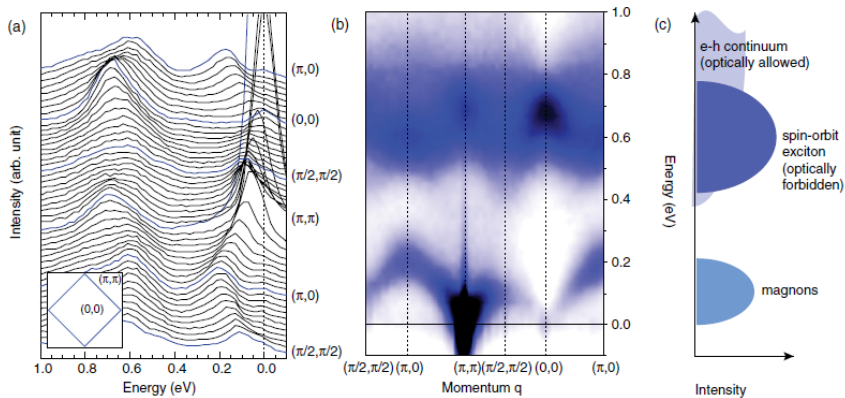
"Resonant inelastic x-ray scattering," P.M. Platzman and E.D. Isaacs, *Phys. Rev. B* **57**, 11108 (1998)

RIXS measures electronic excitations



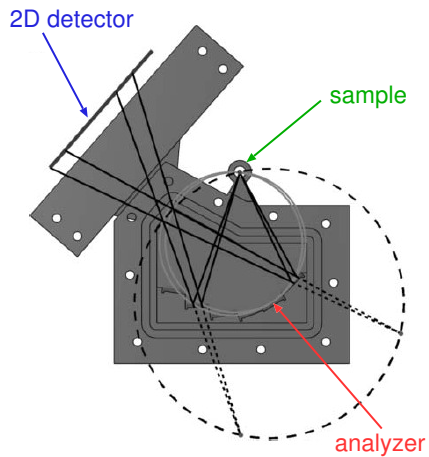
"Resonant inelastic x-ray scattering," P.M. Platzman and E.D. Isaacs, *Phys. Rev. B* **57**, 11108 (1998)

RIXS example

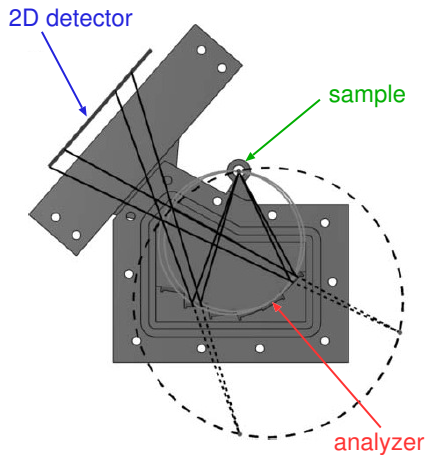


"Magnetic excitation spectra of Sr_2IrO_4 probed by resonant inelastic x-ray scattering: Establishing links to cuprate superconductors," J. Kim, D. Casa, M.H. Upton, T. Gog, Y.-J. Kim, J.F. Mitchell, M. van Veenendaal, M. Daghofer, J. van den Brink, G. Khaliullin, and B.J. Kim, *Phys. Rev. Lett.* **108**, 177003 (2012).

X-ray emission spectroscopy (XES)

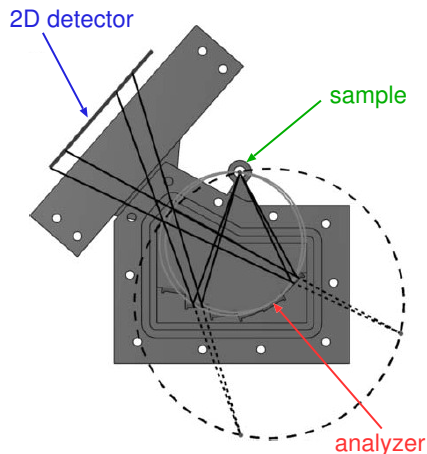


X-ray emission spectroscopy (XES)



Normally a fluorescence line is measured with a detector which cannot resolve its fine structure

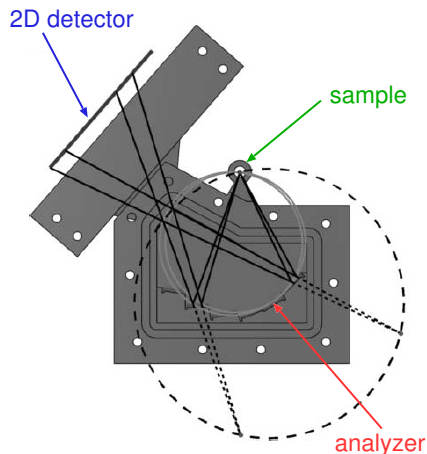
X-ray emission spectroscopy (XES)



Normally a fluorescence line is measured with a detector which cannot resolve its fine structure

with an XES analyzer, the fine features of the emission spectrum are separated

X-ray emission spectroscopy (XES)

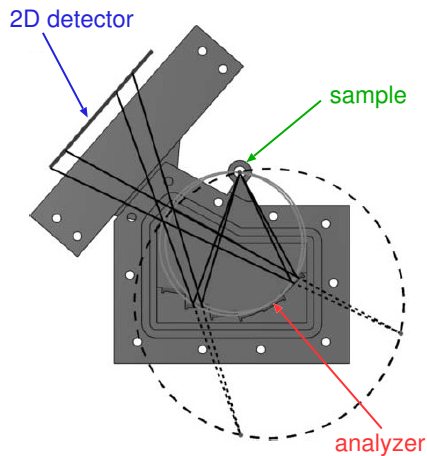


Normally a fluorescence line is measured with a detector which cannot resolve its fine structure

with an XES analyzer, the fine features of the emission spectrum are separated

the analyzer crystal diffracts different energies at different angles, spreading the different energies over the face of the 2D detector

X-ray emission spectroscopy (XES)



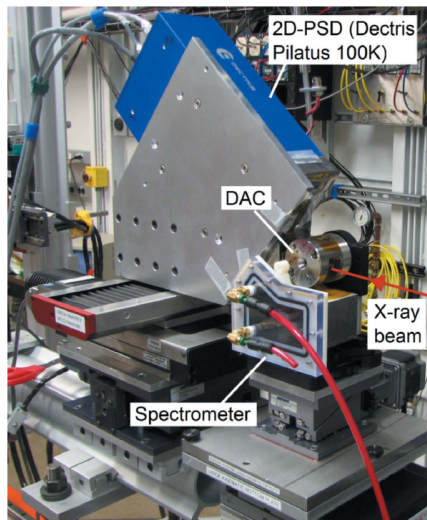
Normally a fluorescence line is measured with a detector which cannot resolve its fine structure

with an XES analyzer, the fine features of the emission spectrum are separated

the analyzer crystal diffracts different energies at different angles, spreading the different energies over the face of the 2D detector

each crystal in the analyzer collects the same range of fluorescence energies for a larger solid angle

X-ray emission spectroscopy (XES)



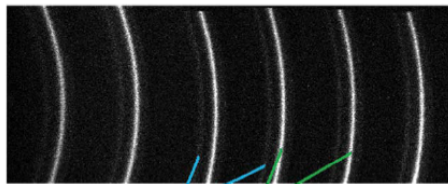
Normally a fluorescence line is measured with a detector which cannot resolve its fine structure

with an XES analyzer, the fine features of the emission spectrum are separated

the analyzer crystal diffracts different energies at different angles, spreading the different energies over the face of the 2D detector

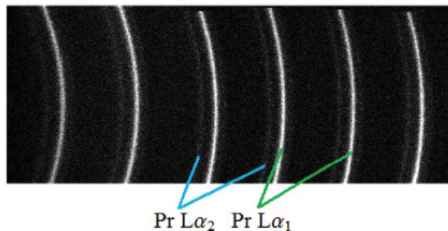
each crystal in the analyzer collects the same range of fluorescence energies for a larger solid angle

RIXS spectrometer performance



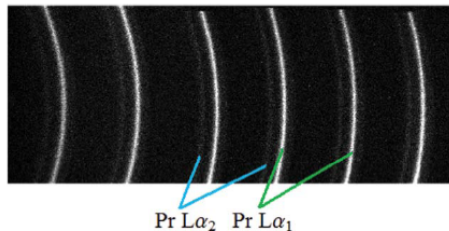
Pr $L\alpha_2$ Pr $L\alpha_1$

RIXS spectrometer performance



The Pr-containing sample is placed in a diamond anvil high pressure cell (DAC) and illuminated with energies near the Pr L_3 edge (5964 eV)

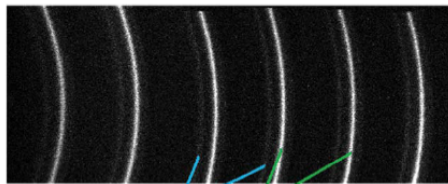
RIXS spectrometer performance



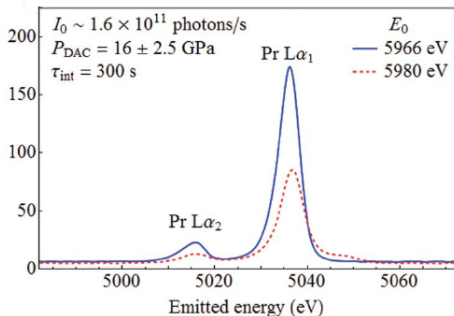
The Pr-containing sample is placed in a diamond anvil high pressure cell (DAC) and illuminated with energies near the Pr L₃ edge (5964 eV)

the spectrometer clearly separates the Pr L α_1 (5035.2 eV) and L α_2 (5015.7 eV) emission lines

RIXS spectrometer performance



Pr $L\alpha_2$ Pr $L\alpha_1$



The Pr-containing sample is placed in a diamond anvil high pressure cell (DAC) and illuminated with energies near the Pr L_3 edge (5964 eV)

the spectrometer clearly separates the Pr $L\alpha_1$ (5035.2 eV) and $L\alpha_2$ (5015.7 eV) emission lines

after integration, the two peaks can be seen to change relative intensities and even position as a function of the incident energy: just at the absorption edge and 14 eV higher